

DAMAGE EVOLUTION AND DAMAGE TOLERANCE IN CERAMIC MATRIX COMPOSITES: EMPIRICAL MEASUREMENTS AND ANALYTICAL/NUMERICAL MODELING

Michael G. Jenkins

Department of Mechanical Engineering, University of Washington
Mechanical Engineering Building, Box 352600, Stevens Way
Seattle, WA 98195-2600

ABSTRACT

Ceramic matrix composites (CMCs) and continuous fibre ceramic composites (CFCCs) were developed to possess the desirable attributes of monolithic ceramics while exhibiting inherent damage tolerance through nonlinear energy absorption mechanisms. Empirical measurements and mathematical (analytical and numerical) models of this damage absorption have contributed to understanding the thermo-mechanical behaviour of CMCs. From this understanding have developed better test methods, greater predictive modeling capability of material behaviour, more appropriate processing methods, and finally design methods for utilizing CMCs. This paper presents background on CMC damage, discusses damage measurement and damage models and finally alludes to the role of damage mechanics in future developments/uses of CMCs.

KEYWORDS

ceramic matrix composites, damage tolerance, damage mechanics, modeling, testing

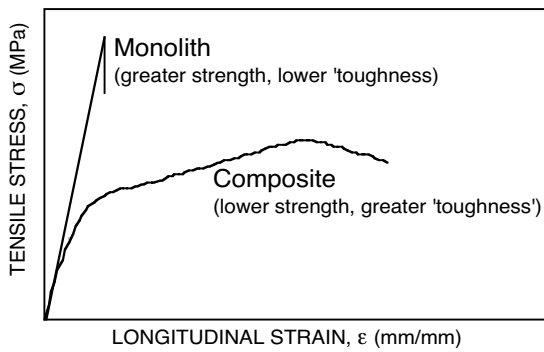
INTRODUCTION

Ceramic Matrix Composites

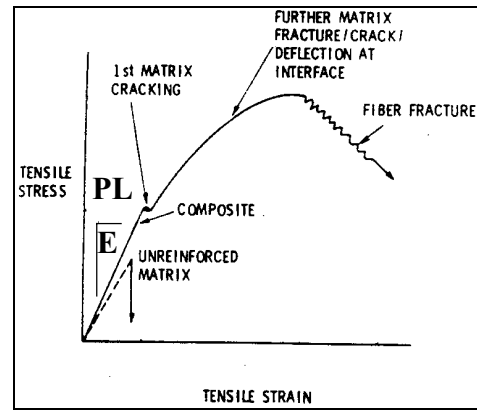
Ceramic matrix composites (CMCs) comprise a maturing subset of the broader genre of engineering materials known as composites. CMCs have potential applications in advanced engineering applications because they possess ceramic materials' high-temperature strengths, corrosion/erosion resistances, high stiffnesses, and low densities, while avoiding the brittle, catastrophic failure preventing monolithic ceramics' acceptance in modern designs [1]. In particular, for those CMCs 'reinforced' with continuous fibres, the synergistic micromechanical interaction of fibers, fiber coatings (a.k.a., interphase), matrix, and overcoats give these CMCs much greater resistance to catastrophic failure than for monolithic ceramics.

Because fibre-reinforced CMCs possess greater 'toughness' (i.e., energy absorption without catastrophic failure macroscopically measured as the area under the tensile stress-strain curve) they exhibit increased reliability and damage tolerance. While these CMCs offer greater 'toughness' than monoliths, their strengths can be much less (see Figure 1), thus necessitating still-evolving and different approaches to mechanical design with CMCs. Despite this limitation, numerous industrial, power generation and aerospace uses have been identified for CMCs including filters, heat exchangers, combustor liners, vanes, and nozzles [1].

It is important to note that design of and design with advanced materials are distinct but not always separate areas of modern engineering efforts. Early CMCs were discouragingly 'not tough' because micro mechanisms that lead to successfully 'tough' and damage tolerant materials were not well understood or appreciated. Eventually, mechanicians identified micro mechanisms and developed mathematical models [e.g., 2-11] such that design of modern CMCs now includes predictive micromechanical models to develop 'tough' high performance materials. Furthermore, significant strides have been made in CMC standard test



a) Comparison of stress-strain curves



b) Details of stress-strain curve for CMC

Figure 1: Engineering stress-strain curves for monolithic and composite (CMC) ceramics

methods [12] with rudimentary design/codes [13] for CMCs now being implemented. These strides have allowed engineers to begin introducing well-designed CMCs in trial, short-term applications. The next major step yet to be achieved in utilizing CMCs is to understand and accommodate long-term behaviour.

As a starting point for long-term predictive design tools, it is useful to examine a CMC quasi-static tensile engineering stress strain curve (Figure 1b). Although Figure 1b is representative of many CMCs and appears quasi-ductile (linear region followed by a nonlinear region before peaking at the ultimate tensile strength, UTS), there is a critical difference between the behaviors of CMCs and those of ductile metals. Specifically, in CMCs the onset of nonlinearity (a.k.a., proportional limit, PL) does not represent the yield point and onset of work hardening as it does in ductile metals. In CMCs the PL is associated with the macro-manifestation of first matrix cracking (or crack opening) and onset of the cumulative damage process.

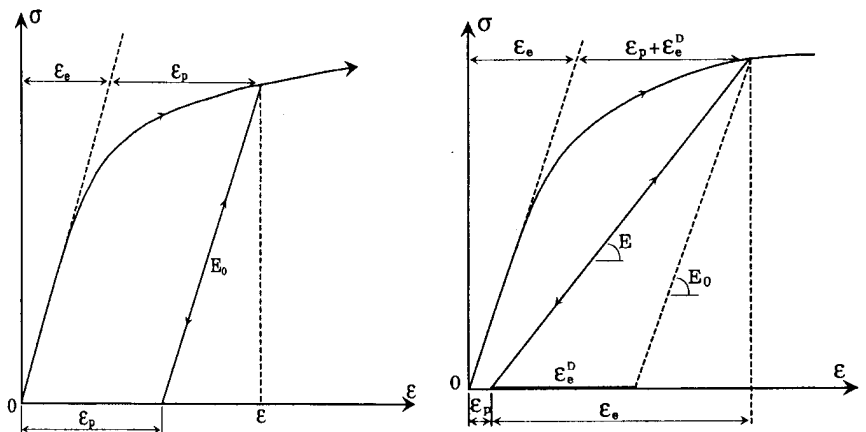
The still-evolving design codes for CMCs [13] have yet to describe how engineers are to account for the PL. One approach adopts conventional static failure theories based on ‘yield’ that dictates, for example comparing the stress state, σ_h , to the PL through a factor of safety, FS, such that $FS = PL / \sigma_h$. (note that $FS > 1$ for a ‘safe design’). Although this conservative approach exploits only the linear regime of material behaviour, it addresses neither long-term behaviour/durability or the lauded damage tolerance of CMCs.

Continuum Damage Mechanics

The cumulative damage of CMCs, whether in the short-term nonlinear stress-strain curve (Figure 1) or over long periods times (e.g., creep deformation or cyclic fatigue failure) is a progressive physical process during which the matrix cracks, the interphase shears, and fibres fracture. Continuum damage mechanics (CDM) is the study, through thermo-mechanical variables, of the deterioration of the continuum of material [14, 15]. CDM does not require individual failure mechanisms, but rather it includes the response of the bulk material.

At the microscale, deterioration of the continuum is the accumulation of micro stresses and strains at defects or interfaces and the initiation and growth of microcracks. At the mesoscale of a representative volume element, the growth and coalescence of these microcracks can form a single crack. At the macroscale, the single crack can propagate to cause final fracture. Damage variables and CDM can be used to describe material behaviour at the microscale and mesoscale while fracture mechanics can be used at the macroscale.

In applying CDM, it is important to distinguish between corresponding consecutive states of the material: deformation, damage and crack propagation. The irreversible deformation of plasticity is not complete (Figure 2a), because the material can be ‘re-deformed’ to restore its original shape/state. However, damage corresponds to material degradation. Complete deformation is comprised of a negligible plastic component plus combined damage and elastic components (Figure 2b). The damage



a) Plastic and elastic deformation

b) Plastic, elastic and damage deformation

Figure 2: Stress-strain response due to a) plastic and elastic deformation and b) plastic, elastic and damage deformation [16]

component contributes to decreased elastic modulus and inability to return the material to the original state by ‘re-deformation’ [16].

The evolution of design and analysis philosophies indicates that use of damage tolerance (e.g., CDM) is a recent occurrence [15]. For example, in aircraft design, methods involving static strength spanned ~1900 to 1950, safe life (a.k.a., fatigue crack initiation) methods spanned ~1950 to 1960, fail-safe life (fatigue crack detection and accommodation) methods spanned ~1960 to 1975, and damage tolerant (residual strength, rate of damage growth, damage detection, and CDM) spanned the time from ~1975 to present.

It is interesting to note that the maturation of CMCs and CDM have occurred concurrently (~1970’s to present). However, the applications of the concepts of CDM to CMCs have been limited even though the quasi-brittle behaviour of CMCs makes them an apparently ideal candidate for CDM-based analyses. In the following sections, some examples of the applications of CDM concepts to CMCs are described first for damage measurements then for damage models (both analytical and numerical).

DAMAGE MEASUREMENTS

Having described the concept of damage mechanics, it is useful to describe methods for actually measuring damage in materials. Four types of measurements have been identified [16]: a) Measurement of remaining life (e.g., cycles to failure in fatigue, time to failure in creep, etc.); b) Microstructural measurements (e.g. volume fraction of defects, cavities, microcracks, etc.); c) Measurement of physical parameters (e.g., density, resistivity, acoustic emission, etc.); and d) Measurement of mechanical behaviour (e.g., change in elastic modulus, etc.)

For mechanical modeling of damage, measurements of mechanical behaviour are best. Two approaches to assess mechanical behaviour of damage have been used for determining stress: net stress based on the net section and effective stress that accounts for stress concentration near defects. For the uniaxial case, the net stress is $\sigma^* = \sigma / (1 - \omega)$ [16] where σ = true normal stress and ω = average reduction in section area due to microcracks and voids. The effective stress is $\tilde{\sigma} = \sigma / (1 - D)$ [16] where D is macroscopic damage.

The variation in mechanical behaviour can be measured through the variation of application-specific parameters. For example, variation in elastic modulus, E, is used such that $D = 1 - (\tilde{E} / E)$ where \tilde{E} is the actual damaged elastic modulus. Similarly variation of microhardness, H, can be used such that $D = 1 - (\tilde{H} / H)$ where \tilde{H} is the actual damaged microhardness. A summary (Figure 3) of the ‘quality’ of physical and mechanical damage measurement methods/parameters has been given by Lemaitre [14].

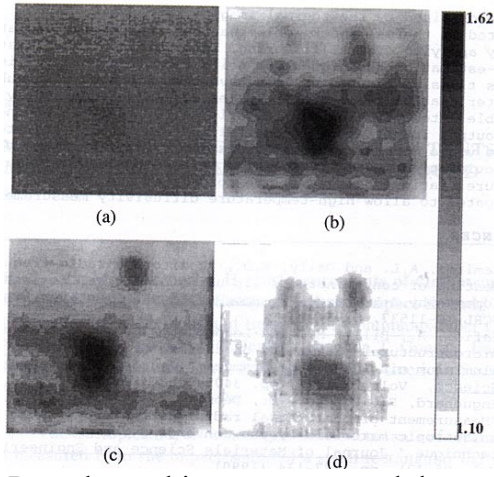
An example of the use of a nondestructive characterization (NDC) method applied to assess damage is shown in Figure 4 for a CMC. An infrared measurement system coupled to laser flash excitation method was used to measure thermal diffusivity as a function of power generation use time [17]. Variation in grayscale (Figures 4a-4d) can be linked to through-thickness variation in thermal diffusivity (i.e., loss of structural integrity or damage). Change of thermal diffusivity with thermal cycles is shown in Figure 4e.

Acoustic emission (AE) can be linked to damage evolution in CMCs. During monotonic and/or cyclic loading of CMC test specimens, the ‘number of counts’ from the AE system is related to 1) onset of nonlinearity (e.g., matrix cracking) and 2) increasing nonlinearity (continued matrix cracking and fibre fracture) of the stress-strain curve. The unload/reload stress-strain curves (Figure 5a) and the AE cumulative counts vs stress (Figure 5b) show this relationship between nonlinearity and damage for a CMC.

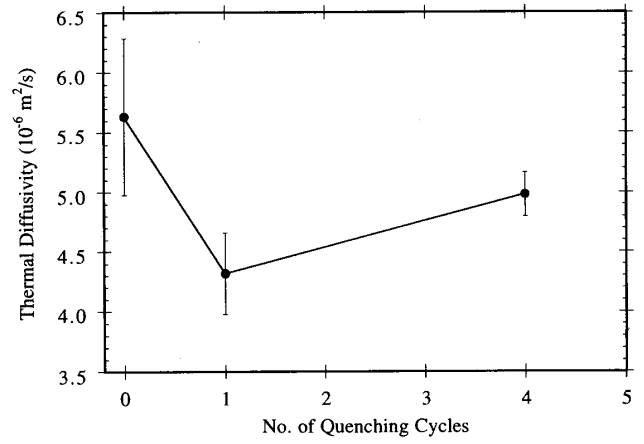
An example of a newly proposed mechanically-based damage parameter for CMCs based on slope and energy information from the monotonic tensile stress-strain curve is given by [19]:

Mechanical/Physical Parameter	Damage Parameter	Brittle	Ductile	Creep	Low cycle fatigue	High cycle fatigue
Micrography	$D = 1 - (\partial S_D / \partial S)$	Try to see	Good	Good	Try to see	Try to see
Density	$D = 1 - (\bar{\rho} / \rho)^{2/3}$	Do not try	Good	Try to see	Try to see	Do not try
Elastic Modulus	$D = 1 - (\tilde{E} / E)$	Good	Very good	Very good	Very good	Do not try
Ultrasonic Wave	$D = 1 - (\tilde{V}_L^2 / V_L^2)$	Very good	Good	Good	Try to see	Try to see
Cyclic Stress Amplitude	$D = 1 - (\Delta\sigma / \Delta\sigma^*)$	Do not try	Try to see	Try to see	Good	Try to see
Tertiary Creep	$D = 1 - (\dot{\epsilon}_p^* / \dot{\epsilon}_p)^{1/N}$	Do not try	Try to see	Very good	Try to see	Do not try
Micro-Hardness	$D = 1 - (\tilde{H} / H^*)$	Good	Very good	Good	Very good	Try to see
Electrical Resistance	$D = 1 - (V / \tilde{V})$	Try to see	Good	Good	Try to see	Try to see

Figure 3: ‘Quality’ chart of methods of damage measurement [14]



a-d) Raw thermal image, processed thermal image, diffusivity image, and enhanced diffusivity image, respectively.



e) Effect of number of quench cycles ($\Delta T=800^\circ\text{C}$)

Figure 4: Infrared imaging to assess damage in a SiC fibre-reinforced SiC matrix CMC [17]

$$\tilde{D}(\sigma_i) = \left(1 - \frac{(d\sigma_c/d\varepsilon_c)_i}{(d\sigma_c/d\varepsilon_c)_0} \right) \left(\frac{U_{p,i}}{U_p^*} \right) \quad (1)$$

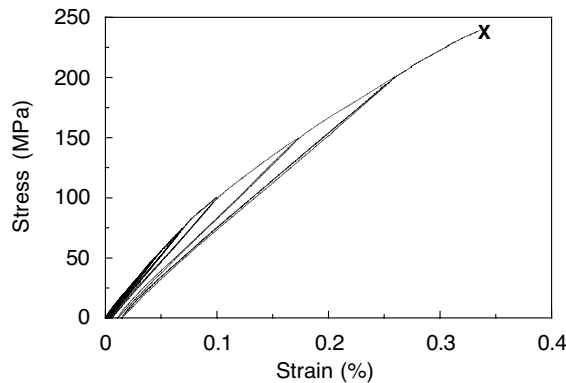
where $(d\sigma_c/d\varepsilon_c)_i$ is the tangent modulus at i -th point in the monotonically-loaded tensile stress-strain (σ_c - ε_c) curve, (for i -th stress, σ_i , and strain, ε_i), $(d\sigma_c/d\varepsilon_c)_0$ is the tangent modulus in the linear region of the tensile stress-strain curve where $(d\sigma_c/d\varepsilon_c)_0 \approx E_0$, $U_{p,i}$ is inelastic energy absorption at σ_i during the tensile test and U_p^* is the inelastic portion of the total energy absorption during the tensile test just up to the UTS, σ_{cu} .

Figure 6 compares D from Equation 1 to the simple model based on $D=1-(\tilde{E}/E_0)$ where \tilde{E} is the tangent modulus using the monotonic stress-strain tensile stress curves of a CMC. D determined from Equation 1 reflects the rapidly increasing cumulative damage as the nonlinearity of the stress-strain curve increases whereas the simple damage model based on elastic modulus seems to have a series of plateaus.

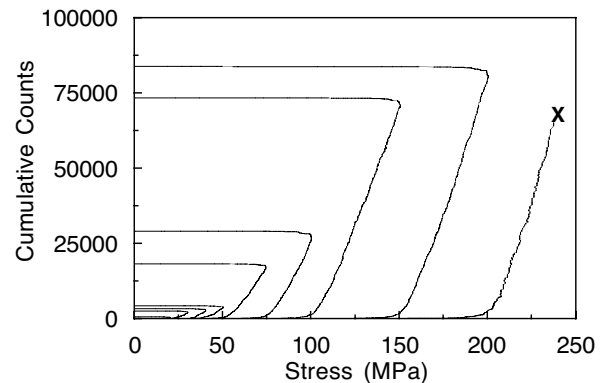
DAMAGE MODELS

Analytical

CDM has been developed generally along the concepts of the theory of irreversible processes with internal variables. Total strain is divided into the sum of elastic, plastic and thermal expansion strains from which the elastic and thermal strains are combined into a single reversible, thermoelastic strain (i.e. a state variable). From the total observed strain and the temperature, the local state method develops the framework of CDM from the thermodynamic state of material. The first principle of thermodynamics expresses energy conservation while the second principle of thermodynamics expresses the irreversibility of the entropy production giving an interpretation of the energies stored as heat or stored in the material (see Figure 7). Note that the energy stored by hardening corresponds to an increase in free energy (i.e. internal energy) whereas the energy dissipated by damage is lost by the material (i.e., irreversible decrease in free energy).



a) Unload/reload stress strain curve

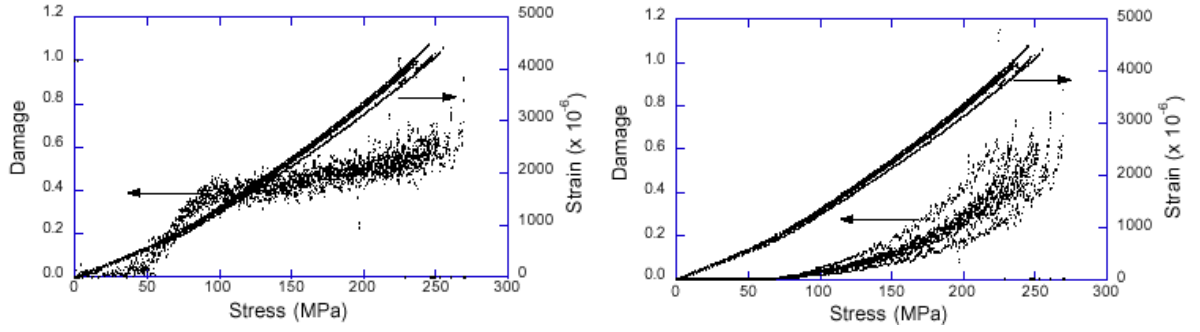


b) Cumulative AE counts for hysteresis loops

Figure 5: Correspondence of AE cumulative counts and the nonlinearity of the stress-strain curves for a SiC fibre-reinforced SiC matrix CMC [18]

From these bases, many 'special' case isotropic CDM models have been introduced for damage equivalent stress

(plasticity and viscoplasticity) and strain damage (plasticity and viscoplasticity).



a) Damage=f(tangent modulus) only b) Damage=f(tangent modulus and inelastic energy)

Figure 6: Comparison of damage parameters and strain-stress curves for a Si-C-O fibre reinforced Si-C-N-O matrix CMC [20]

For CMCs, anisotropic material damage models include maximum principal stress, 2nd order damage tensor, 4th order damage tensor, and double scalar variable. One such example includes [17]:

$$\Psi = \frac{1}{2} \left\{ \{\varepsilon\} - \{\varepsilon^p\} \right\} [C_o] \left\{ \{\varepsilon\} - \{\varepsilon^p\} \right\} + \frac{1}{2} \left\{ \{\varepsilon\} - \{\varepsilon^c\} \right\} [\Delta C^{eff}] \left\{ \{\varepsilon\} - \{\varepsilon^c\} \right\} \quad (2)$$

and

$$\{\sigma\} = \frac{\partial \Psi}{\partial \{\varepsilon\}} = [C_o] + [\Delta C^{eff}] \left\{ \{\varepsilon\} - \{\varepsilon^c\} \right\} + [C] \left\{ \{\varepsilon^c\} - \{\varepsilon^p\} \right\} \quad (3)$$

where Ψ = free energy, $\{\varepsilon\}$ = total strain vector, $\{\varepsilon^p\}$ = plastic strain vector, $\{\varepsilon^c\} = \{\varepsilon\} - \{\varepsilon^p\}$,

$[C_o]$ = undamaged stiffness matrix, $[\Delta C^{eff}]$ = damaged, reduced stiffness matrix, $\{\sigma\}$ = stress vector

Employing a hierarchical approach (e.g., Equations 2 and 3) along with constitutive constants from uniaxial tension and compression tests the multiaxial damaged stress-strain response of a CMC was predicted using strain as the independent state variable. The modeling is sophisticated but has been implemented in industrial design codes, with good agreement with actual experimental results for this CMC (see Figure 8).

Numerical

Many examples of numerical damage models could be related. These models may be as direct as applying linear damage models sequentially (e.g., Miner's Rule) or as involved as those that employ finite element analysis (FEA) programs 'drive' the accumulation of damage. Two FEA examples follow.

FEA model of an unnotched beam

In this study [21], a double meshed (i.e., one set of nodes, but two sets of elements, fibre and matrix) FEA model was constructed of a flexure test specimen geometry that had been used to strength test a three-dimensionally braided CMC [22]. A macrocode was written for the commercial FEA code such that matrix or fibre elements were 'killed' if the maximum principal stress in the respective elements exceeded the UTS of the respective materials. Good agreement between empirical and numerical results is shown in Figure 9. Note that most matrix elements have failed by the test's end, leaving only fibre elements to carry the load.

FEA model of a notched beam

In this study [23], an FEA model with macrocode was constructed using the same double meshing procedure and methodology [21, 22]. A single edge notched beam was modeled to compare the numerical results to R-curve behaviour in a unidirectionally-reinforced CMC. In this case matrix elements substantially failed not only near the notch tip but also distributed in the CMC. Fibres failed only near the notch region.

DISCUSSION AND CONCLUSIONS

Nonlinear monotonic tensile stress-strain curves are speculative and analytical foci used to describe the mechanical behaviour of CMCs and attendant micromechanics. In attempts to describe and extract additional information from these tensile tests, such methodologies as unload/reload tensile tests [e.g.,24-27] have been proposed. These methodologies provide information about in-situ mechanical properties of constituent materials but still require detailed knowledge and modeling of the micromechanics.

CDM, although a relative 'newcomer' for describing the mechanical properties and performance of CMCs, has the major advantage of simplifying the analysis of mechanical behaviour by reducing the requirements

$$\boxed{\begin{array}{c} W_{ch} \\ \text{(energy dissipated} \\ \text{as heat)} \end{array}} = \boxed{\begin{array}{c} W_p \\ \text{(supplied} \\ \text{irreversible energy)} \end{array}} - \boxed{\begin{array}{c} W_a \\ \text{(energy stored by} \\ \text{hardening)} \end{array}} + \boxed{\begin{array}{c} W_{ch} \\ \text{(energy dissipated} \\ \text{by damage)} \end{array}}$$

Figure 7: Illustration of the dissipation during plastic flow/deformation and damage [17]

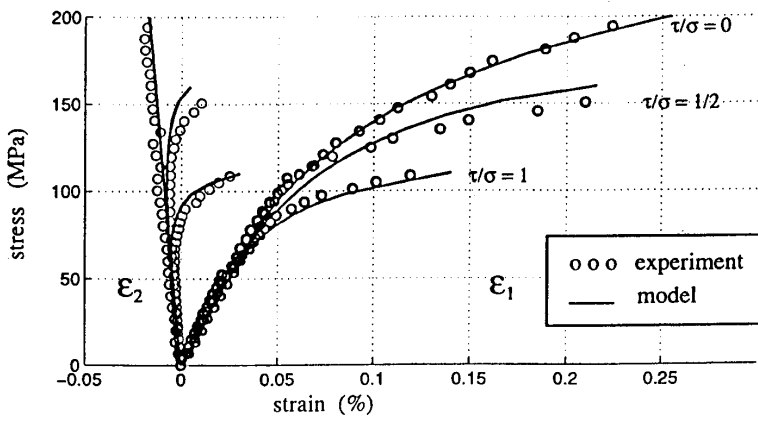


Figure 8: Comparison of experimental and damage model prediction results for a SiC fibre / SiC matrix CMC [16]

for knowledge about the individual micro mechanisms of failure and properties and performance of the constituent materials. CDM describes the cumulative damage process inherent in quasi-brittle CMCs as reflected by their nonlinear stress-strain curves and fracture surfaces.

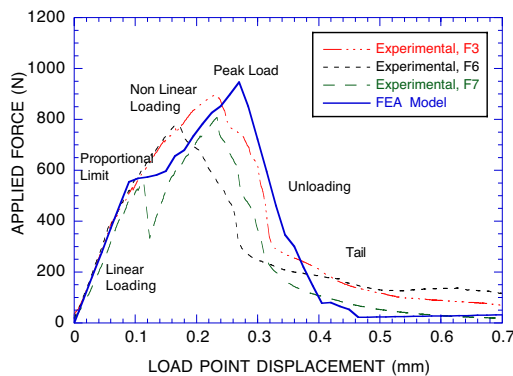
In applying CDM to CMCs under ambient conditions, both analytical and numerical approaches have successfully described mechanical behaviour in complex stress states. With modifications, time/environmental aspects of constituent materials and bulk CMCs can be integrated into the damage models to describe long-term durability.

ACKNOWLEDGEMENTS

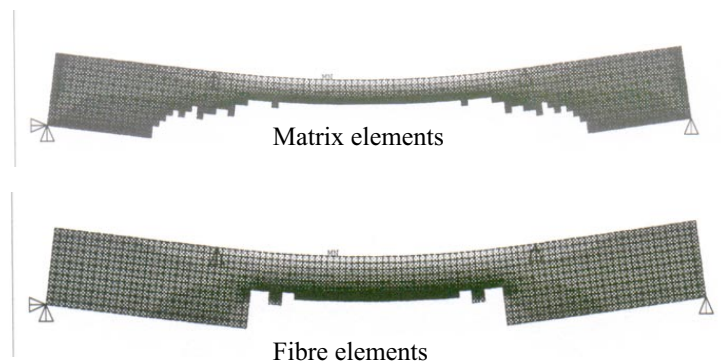
This work was sponsored by the U.S. Department of Energy, Assistant Secretary for Energy Efficiency and Renewable Energy, Office of Industrial Technologies, Industrial Energy Efficiency Division and Continuous Fiber Ceramic Composites Program, under contract DE00OR22725 with UT-Battelle, LLC.

REFERENCES

1. Karnitz, M.A., Craig, D.A., Richlen, S.L. (1991) *Ceram. Bull.*, 70, 430.
2. Aveston, J., Cooper, G.A., Kelly, A. (1971) In, *The Prop of Fibre Comp*, NPL, IPC Press, Teddington, U.K., 15.
3. Rice, R. W. (1981) *Ceram. Eng., Sci Proc.* 2, 661.
4. Marshall, D.B., Cox, B.N., Evans, A.G. (1985) *Acta Metall.*, 33, 2013.
5. Rice, R. W., (1985) *Ceram. Eng., Sci Proc.* 6, 589.
6. Budiansky, B., Hutchinson, J.W., Evans, A.G. (1986) *J. Mech. Phys. Solids*, 34, 167.
7. McCartney, L.N. (1987) *Proc. R. Soc. London, A.*, 409, 329-350.
8. Evans, A. G., Marshall, D. B. (1989) *Acta Metall.* 37, 2567.
9. Curtin, W. A. (1991) *J. Amer. Ceram Soc.*, 74, 2837.
10. Inghels, E, Lamon, J. (1991) *J. Mater. Scienc.* 26, 5403 and 5411.
11. Evans, A. G., Zok, F. W. (1994) *J. Mat. Scienc.* 29, 3857.
12. Jenkins, M. G. (1999) *Advanced Composite Materials*, 8, 55.
13. CMCs, Vol 5, MIL-HDBK-17, (Yellow Pages) (2000) DoD Handbook, Secretariat: MSC, Fort Wash., Penn..
14. Lemaitre, J. (1996) *A Course on Damage Mechanics*, Springer Verlag, Berlin.
15. Krajcinovic, D. (1996) *Damage Mechanics*, Elsevier, Amsterdam.
16. Chaboche, J.-L. (1999) In, *Creep & Damage in Materials & Structures*, Springer-Verlag, New York, 209.
17. Ahuya, S., Ellingson, W.A., Steckenrider, J. S., (1997) In, STP 1309, ASTM, W. Conshohocken, Penn., 209.
18. Jenkins, M.G., Piccola, J.P. Jr., Lara-Curzio, E. (1996) In, *Frac Mech of Ceramics*, Plenum, New York, 267.
19. Mamiya, T. Kagawa, Y., Jenkins, M.G. (2001) In, *Proc. 2001 SEM Annual Conf*, SEM, Bethel, Conn., 566.
20. Kessler, B. S., Jenkins, M.G. (2001) In, *Proc. 2001 SEM Annual Conf.*, SEM, Bethel, Conn., 430.
21. Jenkins. M.G., Mark. K.Y. (2001) *J. Materials Design and Analysis*, in press.
22. Jenkins, M.G., Mello, M.D. (1996) *Mater. Manuf. Processes*, 11, 99.
23. Kwon, O.H., Jenkins, M. G., (2001) Univ. of Wash. Report.
24. Burr, A., Hild, F., Leckie, F. A. (1997) In, STP 1315, ASTM, W. Conshohocken, Penn.
25. Evans, A. G., Domergue, J.-M., Vagaggini, E., (1994) *J. Am. Ceram. Soc.*, 77, 1425.
26. Steen, M., Valles, J. L., (1996) In, , STP 1309, ASTM, W. Conshohocken, Penn, 49.
27. Campbell, C. X., Jenkins, M. G., (2000) In, STP 1392, ASTM, W. Conshohocken, Penn, 118.



a) Load-displacement results



b) 'Unkilled' elements at end of test

Figure 9: Results of FEA modeling of a CMC four-point flexure test specimen using element 'kill' commands for a 3-D braided SiC fibre reinforced SiC matrix CMC